

Orientation changes during the cold drawing and subsequent annealing of PEEK*

D. J. Blundell†, A. Mahendrasingam‡§, D. McKerron†, A. Turner‡, R. Rule††, R. J. Oldman†† and W. Fuller‡

†ICI Materials Research Centre, Wilton, Middlesbrough, Cleveland TS6 8JE, UK

‡Macromolecular Structure, Department of Physics, Keele University, Staffordshire ST5 5BG, UK

††ICI Chemicals and Polymers, The Heath, Runcorn, Cheshire WA7 4QE, UK

Two-dimensional wide- and small-angle X-ray scattering (WAXS and SAXS) patterns have been recorded at the Daresbury Synchrotron Radiation Source in time-resolved studies of changes in orientation and crystallinity during annealing of cold drawn samples of poly(aryl ether ether ketone) (PEEK). An amorphous PEEK film drawn uniaxially to a draw ratio of 2.0 was observed to give a well oriented non-crystalline WAXS pattern. The drawn film was then held at constant length and diffraction patterns recorded while the sample temperature was raised at $15^{\circ}\text{C min}^{-1}$ from ambient to the glass transition temperature ($T_g = 145^{\circ}\text{C}$) and beyond. WAXS patterns were recorded with an exposure time of 5 s. Close to T_g there was a sudden loss of orientation so that the diffraction pattern resembled that given by the specimen before cold drawing. This absence of crystallinity and orientation persisted for ~ 45 s after which the unoriented non-crystalline pattern began to be gradually replaced by a highly crystalline oriented pattern. This loss of orientation within a non-crystalline specimen close to T_g is consistent with a change from a molecular orientation associated with pseudo-affine deformation to an orientation associated with a stretched rubbery network. From parallel studies, the dramatic changes in the WAXS pattern were found to be correlated with changes in the small angle diffraction. Significant features in the SAXS pattern were not observed until the temperature was $\sim 150^{\circ}\text{C}$ when the meridionally oriented central maximum began to develop. With increasing temperature this maximum gradually broadened in the meridional direction until at $\sim 160^{\circ}\text{C}$ it developed into a distinct meridional peak at a spacing of 140 Å. During subsequent annealing the intensity of this peak increased but its spacing did not change. Also, the half width of this peak in the direction parallel to the equator did not vary during annealing, suggesting that the lateral dimension of the crystalline regions within the specimen does not change during crystallite growth.

(Keywords: synchrotron radiation; time resolved; PEEK)

INTRODUCTION

The effect of physical deformation and annealing on the microstructure and morphology of polymer materials, has been a subject of major technological and scientific interest for a number of years. A principal reason for this is that the production of fibres and films from a thermoplastic polymer commonly involves drawing at a variety of temperatures. Information about this phenomenon can also contribute significantly to fundamental polymer science through an understanding of molecular mechanisms which determine the response of a polymer material to thermal and mechanical stress. Historically, work to this end has necessitated the study of samples from various stages of preparation, using spectroscopic, thermal and mechanical techniques¹⁻³, and has carried the disadvantage of errors introduced by sample-to-sample measurement. In contrast, many benefits such as the observation of subtle behaviour can

be obtained if successive measurements can be carried out on a single changing system⁴. Of the experimental techniques which have now been developed to allow this, time-resolved X-ray diffraction using high intensity synchrotron radiation sources is of particular significance. Reports in the literature reflect an increasing activity in this area and have demonstrated that it is possible to undertake meaningful time-resolved studies during structural transitions in a variety of naturally occurring and synthetic polymer systems⁵⁻⁷. The aim of the present work was to exploit the SERC Daresbury Laboratory Synchrotron Radiation Source (SRS) to explore possibilities for molecular reorganization in the synthetic polymer poly(aryl ether ether ketone) (PEEK) using both wide-angle X-ray scattering (WAXS) (i.e. d spacings from 1 to 50 Å) and small-angle X-ray scattering (SAXS) (i.e. 50–350 Å). These studies led to the observation of short-lived structural transitions not reported in previous X-ray diffraction studies using conventional rotating anode X-ray sources. Finally, in this paper an attempt is made to account for these changes in the diffraction pattern in response to thermal and mechanical stress in terms of models relating chain conformation and chain organization in partially ordered polymer materials.

* Presented at 'Polymer Science and Technology—a conference to mark the 65th birthday of Professor Ian Ward FRS', 21–23 April 1993, University of Leeds, UK

§ To whom correspondence should be addressed

EXPERIMENTAL

Observations were made on strips of PEEK (typically 4 cm long \times 1 cm wide) cut from films of commercially available material originally 100 μm in thickness. WAXS experiments were carried out on beam line 9.6 (wavelength = 0.9 \AA) and SAXS experiments on beam line 2.1 (wavelength = 1.54 \AA) at the Daresbury SRS. Diffraction data on line 9.6 were collected using an Enraf-Nonius FAST detector \sim 64 mm \times 48 mm in area with 65 536 grey levels on 512 \times 512 pixels. This system allowed a complete diffraction pattern to be recorded in 5 s. A series of diffraction patterns recorded in this way can be regarded as successive frames in a continuous record of the variation of the diffraction pattern during the experiment. There was a time delay of 4.7 s between successive frames while each completed frame was downloaded from memory to the hard disc of an on-line VAX computer. Hence diffraction patterns were recorded with a sampling interval of \sim 10 s. The accumulation of each frame could be observed on a VDU in real time. Diffraction data on line 2.1 were collected using a multi-wire proportional counter (MWPC). In both WAXS and SAXS experiments data were collected using a purpose designed camera which allowed uniaxial bi-directional drawing of the specimen and control of its temperature⁸. The strips of PEEK were clamped in the drawing frame of the camera. The rate of drawing could be varied from 0.018 to 1800 mm s^{-1} and draw ratios up to 5.0 were readily achieved. The temperature of the specimen environment could be varied from ambient to 350°C. The temperature close to the specimen was monitored with a thermocouple and could be controlled with an accuracy of 0.5°C.

RESULTS

WAXS patterns from strips of the original sheet of PEEK showed a single broad halo with a maximum intensity at 4.7 \AA spacing, typical of an amorphous organic polymer with essentially no overall preferred orientation in the polymer chains or sufficient regularity in their side-by-side packing to be classed as crystalline. After cold drawing, this halo became concentrated into two equatorial arcs, indicating that there was now significant preferred orientation of the polymer chains. The radial half-width of these arcs was however still comparable to that of the original halo, indicating that the material should still be regarded as non-crystalline.

Two types of WAXS experiment were carried out on previously cold drawn films of PEEK. In the first type of experiment (referred to here as 'continuous') diffraction patterns were recorded while the temperature was continuously increased from ambient to significantly (i.e. 50°C or more) above the glass transition temperature ($T_g = 145^\circ\text{C}$). These experiments showed a sudden loss of orientation above the glass transition which typically persisted for about four or five frames (i.e. \sim 45 s) before the original orientation began to be regained and with it the development of a high degree of crystallinity. These observations prompted a second series of experiments (referred to here as 'interrupted') which took advantage of the capability of the FAST detector to display the diffraction pattern in real time as it accumulated. In these experiments the temperature of the specimen environment was raised as quickly as possible to the temperature (typically within 1°C of 153°C) at which the WAXS

pattern became disoriented and was then held constant during an annealing period in which crystallization occurred. This isothermal crystallization took place on a longer time-scale (typically up to 12 min) than that which was observed in the continuous experiments (typically 1 min).

A selection of WAXS patterns recorded during a typical continuous experiment is shown in Figure 1. The

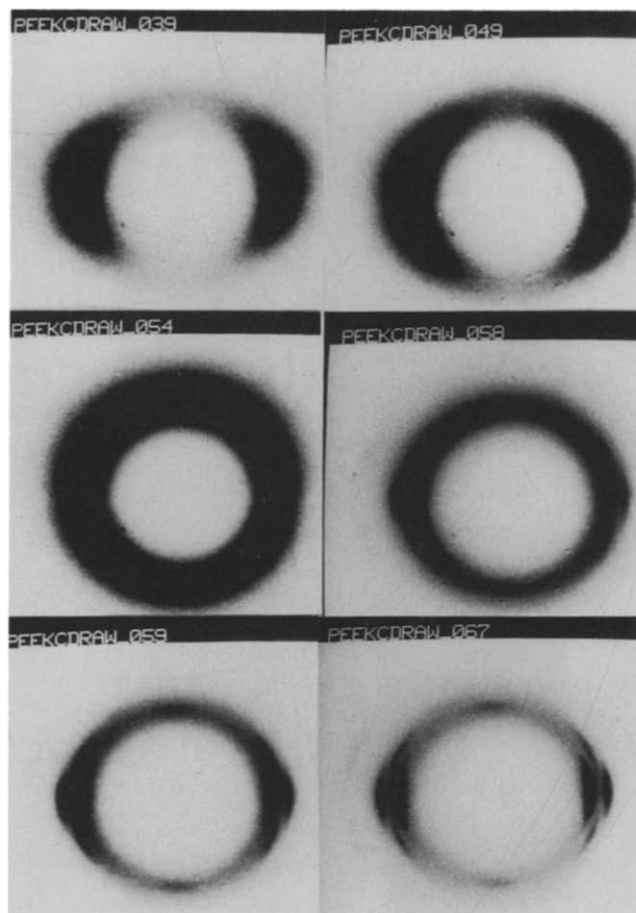


Figure 1 Selected WAXS frames from a continuous type of experiment. The frame number within a sequence of 100 frames is indicated at the top of each frame. Corresponding temperatures are in the text

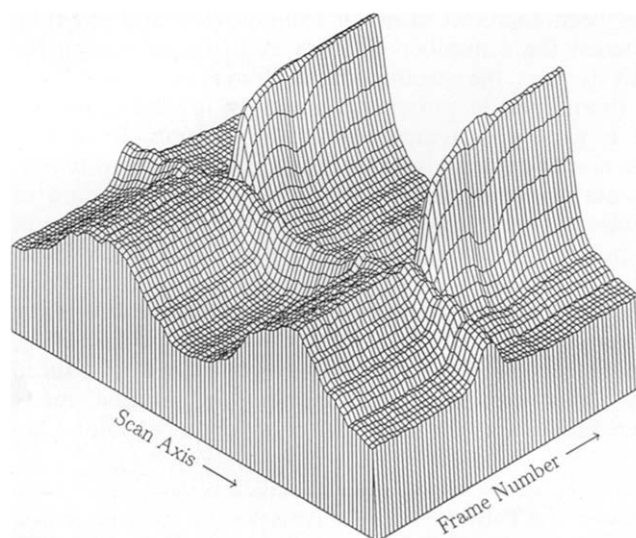


Figure 2 Three-dimensional plot of WAXS azimuthal scans at 4.7 \AA with frame number from 1 to 66 in a continuous type of experiment

initial pattern (frame 39) recorded at 122°C shows the broad equatorial arcs at a spacing of 4.7 Å characteristic of the original cold drawn sample. Frame 49 (142°C) shows an increase in the length of these arcs. In frame 54 (152°C) the loss of orientation is essentially complete. Frame 58 (160°C) shows an early stage in the regaining of orientation and the development of crystalline diffraction on the equator. Frames 59 (162°C) and 67 (178°C) illustrate the further development of orientation and crystallinity. This effect was highly reproducible and *Figure 2* shows a three-dimensional plot of the azimuthal variation in the intensity distribution at 4.7 Å as a function of frame number in a similar experiment to that illustrated in *Figure 1*. The variation at 4.7 Å is of particular interest because in addition to passing through the diffraction halo characteristic of unoriented non-

crystalline PEEK it also monitors the variation in the intensity of the strong {110} reflection from crystalline PEEK. The initial equatorial orientation is readily seen in frames 1 to 24 in *Figure 2* while the temperature increased from 54 to 140°C and its loss can be seen over frames 25 to 31 (142–158°C). In the last of these frames there is an essentially constant intensity distribution. The growth of oriented crystallites is indicated by the appearance of the sharp diffraction from the {110} equatorial reflection which increases rapidly in intensity from frame 32 onward (160–210°C).

A selection of WAXS patterns recorded during a typical interrupted experiment is shown in *Figure 3*. Frame 1 recorded at 52°C shows the original oriented non-crystalline pattern from cold-drawn PEEK. Frames 25 (140°C), 31 (145°C) and 34 (148°C) show a gradual

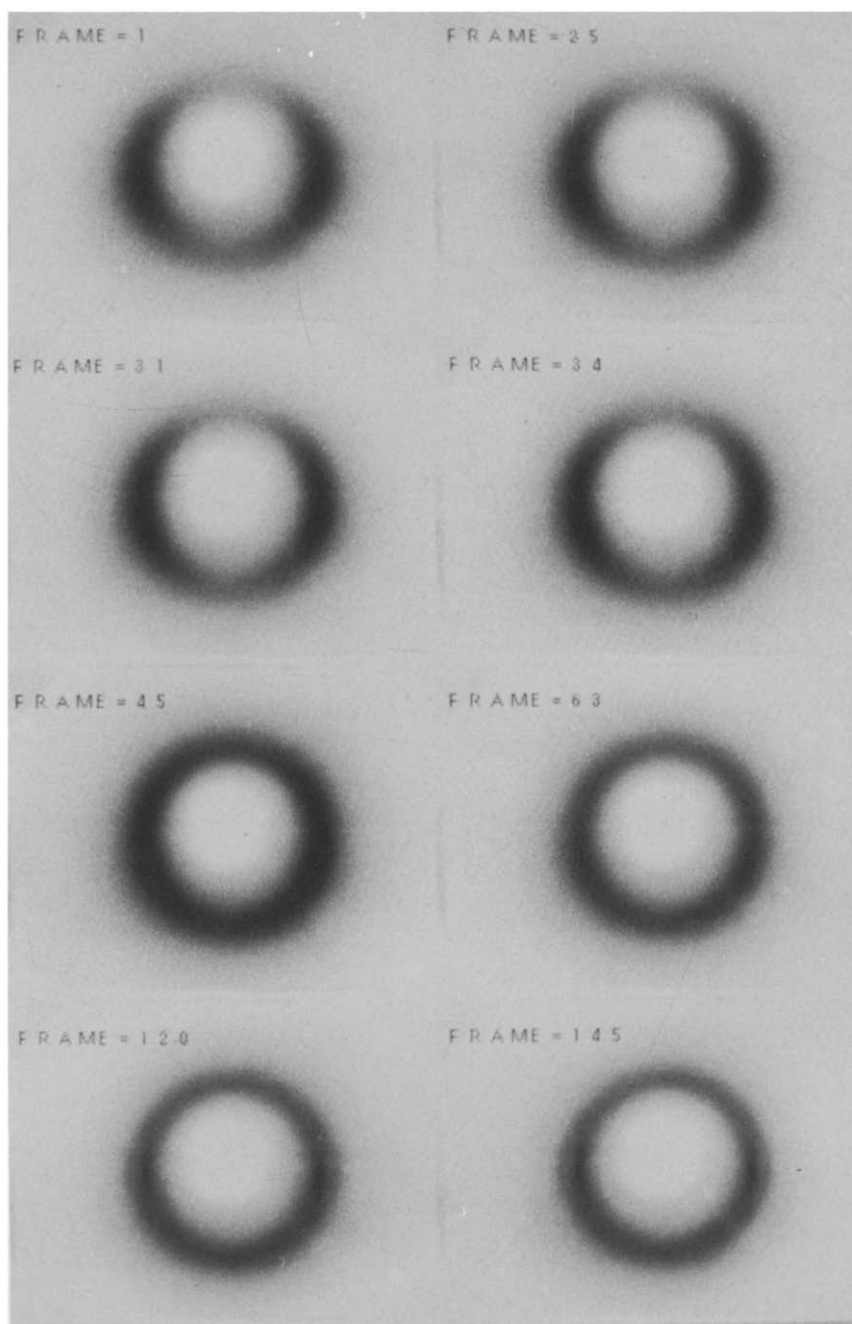


Figure 3 Selected WAXS frames from an interrupted type of experiment. Corresponding temperatures are in the text

loss of this orientation which becomes essentially complete by frame 45 (153°C). The temperature was held at this value during the rest of the experiment. From frames 63, 120 and 145 it can be seen that during this period there was a slow development of crystallization. The crystallites formed in this process could be identified with the crystallites formed in the continuous experiments although the degree of crystallinity was less and the rate of crystallization under these isothermal conditions was slower. The three-dimensional plot of azimuthal scans at a spacing of 4.7 Å in Figure 4 illustrates these changes in orientation and crystallinity during the whole series of frames in this experiment.

The protocol for the SAXS experiments was chosen to parallel as closely as possible that followed in the continuous WAXS experiments. A selection of frames from a typical SAXS experiment are shown in Figure 5. Significant features in the SAXS pattern were not observed until the temperature was $> \sim 140^\circ\text{C}$ (frame 1). By 150°C a meridionally oriented central maximum had begun to develop (frame 8, 154°C). With increasing temperature this maximum gradually broadened in the meridional direction (frame 10, 158°C) until at $\sim 160^\circ\text{C}$ it developed into a distinct meridional peak at a spacing of 140 \AA (frame 12, 162°C). During subsequent annealing while the temperature increased from 166 to 212°C the intensity of this peak increased but its spacing did not change (frames 14, 16, 22 and 34). Also the half width of this peak in the direction parallel to the equator did not vary during annealing, suggesting that the lateral dimension of the crystalline regions within the specimen does not change during crystallite growth. These changes are illustrated quantitatively in Figure 6. Figure 7 illustrates the variation in the profile of the meridional reflection in a direction parallel to the equator during this experiment. This plot shows that despite a very large increase in the intensity of this meridional peak, its half width remains essentially constant over a wide temperature range with a value which corresponds to a lateral correlation of $\sim 100 \text{ \AA}$ for the diffracting entities, although the half width increases at higher temperatures.

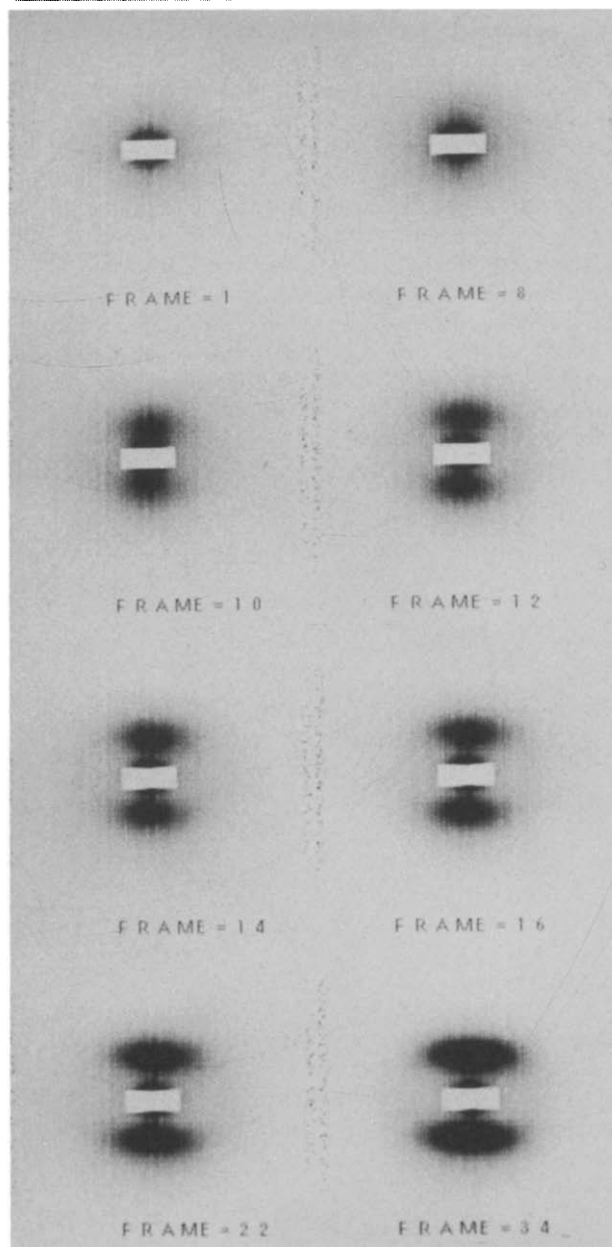


Figure 5 Selected SAXS frames from a continuous type of experiment. Corresponding temperatures are in the text

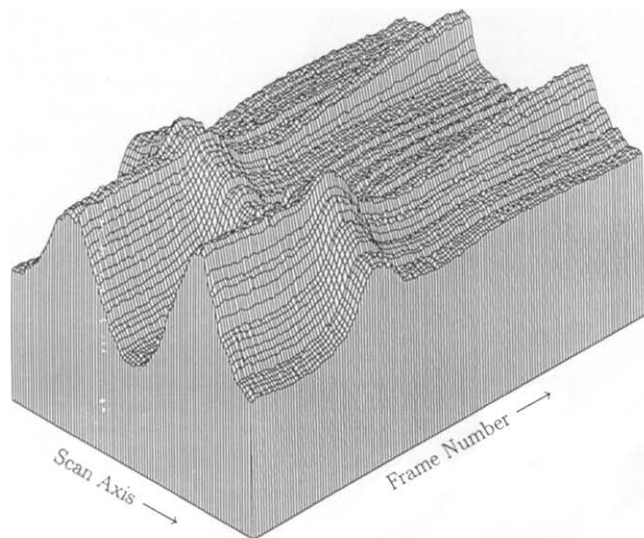


Figure 4 Three-dimensional plot of WAXS azimuthal scans at 4.7 Å with frame number from 1 to 143 in an interrupted type of experiment

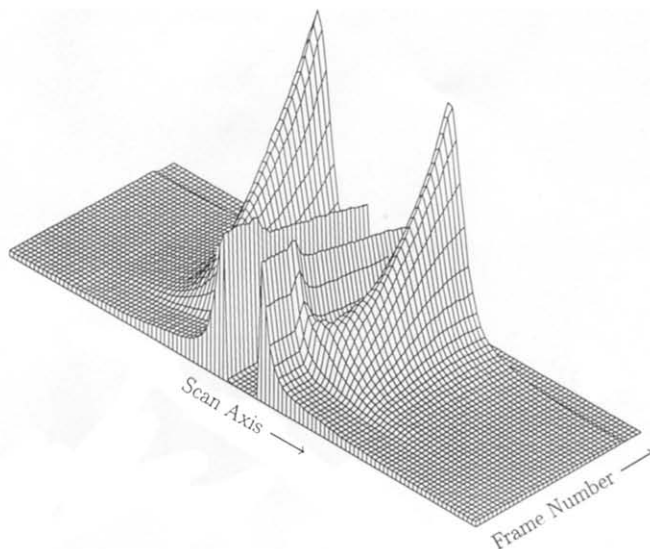


Figure 6 Three-dimensional plot of SAXS meridional scans with frame number from 1 to 40 in a continuous type of experiment

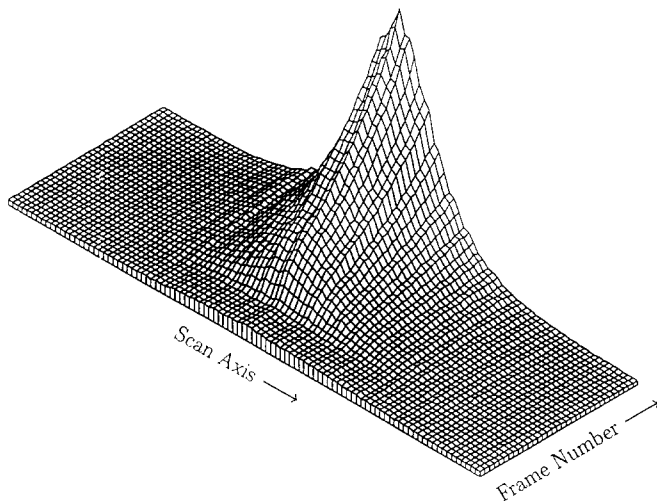


Figure 7 Three-dimensional plot of lateral scans through SAXS diffraction maxima with frame number from 1 to 40 in the same continuous experiment as in Figure 6

DISCUSSION

Origin of the diffraction halo from amorphous and partially ordered polymers

There is no difficulty in understanding the origin of the crystalline reflections observed in the later stages of the continuous and interrupted WAXS experiments. The crystal unit cell of PEEK is well documented in the literature and the reflections observed here are readily accounted for by crystallites with this unit cell oriented so that the polymer chains passing through them parallel to their *c*-axes are aligned predominantly about the draw direction.

The origin of the broad halo and corresponding arcs at 4.7 Å is less straightforward although it is generally accepted that their occurrence in essentially non-crystalline polymers is attributed to interference between scattered radiation from segments of neighbouring chains^{9,10}. Thus it may be assumed that the appearance of equatorial arcs following cold drawing indicates a preferred alignment of chain segments parallel to the draw axis. The azimuthal profile of these arcs can be used to estimate the degree of parallelism of the segment axes^{11–14}. We have used this approach to characterize the changes in the orientation of the segments during drawing and annealing of PEEK.

Models for the deformation of amorphous and partially ordered polymers

In the amorphous state, polymer chains are visualized as interpenetrating each other as they meander along what may be regarded as essentially random paths. Such interpenetrating paths create topographical entanglements that can only be eliminated by the reptation of chains along their paths to allow a chain end to slip through the entanglement¹⁵. Above the polymer T_g , the segments can be assumed to be able to undergo co-operative motion which allows the segments to move past each other. It is this motion that enables chains to reptate and in so doing escape some entanglements and form new ones.

Below T_g , the segments will be dragged along with the changing shape of the solid body. Above T_g , the segments will be able to reorientate independently of the overall

deformation of the body and the chains will be able to adopt new path configurations subject to the constraints of the entanglements. If the temperature is above T_g , such adoption of new path configurations will also depend on the time-scale of the deformation process relative to the reptation of the chains through entanglements. If the deformation is fast, then the entanglements will effectively behave as fixed crosslinks and the chains will be drawn out as in a rubber network. If the deformation is slower, then the chain reptation process will allow the chains to slip past the entanglements.

Two contrasting schemes have been proposed to account for the development of orientation during deformation, both originating from Kuhn and Grun¹⁶. The first approximates the entangled polymer to a crosslinked rubber network where each chain between crosslinks can be represented by freely jointed rigid links and where the crosslinks deform in an affine manner along with the change of deforming body. In this case the chains between the crosslinks are able to adopt new configurations subject only to the constraints of the crosslinks. Roe and Krigbaum¹⁷ have derived an expression for the distribution of segments at an angle θ with respect to the draw direction:

$$w(\cos \theta) = \frac{1}{2} + \frac{1}{4n} (3 \cos^2 \theta - 1) \left(\lambda^2 - \frac{1}{\lambda} \right) \quad (1)$$

where λ is the draw ratio and n is the number of random links per chain.

The second scheme considers the polymer only in terms of an aggregate of the segments that make up the chains. It proposes that the direction of the segment units rotates in a pseudo-affine manner following the direction of lines connecting two points in the deforming body. In this case the segments do not have the ability to reorientate and allow the chains between crosslinks to change configuration. Before orientation, the segments will be randomly oriented at an angle θ' with respect to the draw direction. After a draw ratio λ , then according to the pseudo-affine scheme the segments will be constrained at an angle θ given by:

$$\tan \theta = \lambda^{-3/2} \tan \theta' \quad (2)$$

Subsequent work, particularly by Ward¹⁸, has demonstrated the applicability of these models to polymer deformation, respectively, above and below the T_g . It should be emphasized that, for a given λ , the segment orientation achieved with the pseudo-affine model is significantly higher than with the rubber network model where the segments have the ability to relax. These two models can be used as a basis for understanding the changes in orientation and crystallinity during drawing and annealing of PEEK.

Explanation of time-resolved diffraction

The uniform amorphous diffraction halo indicates that the starting material at room temperature is unoriented. Being below T_g , it can be envisaged as entangled random chains with the segments effectively frozen in position. The drawing process at room temperature will therefore approximate to the pseudo-affine deformation of an aggregate of segments. The topographical entanglements will also deform affinely with the shape of the sample but will have a negligible effect on the rotation of the segments. The strong amorphous diffraction from the segments will be expected to follow the pseudo-affine

rotation process and will concentrate into equatorial arcs as observed for cold-drawn PEEK. Since there is no co-operative motion, the segments will be largely fixed in their directions during the heating at constant length up to the T_g . On reaching the T_g , the onset of co-operative motion will enable the segments to reorient and allow the paths of the chains to move towards configurations that maximize entropy. The structure will therefore quickly move to a state that can be approximated by a deformed rubber network. This will be equivalent to the deformed network that would have been formed if the original deformation had taken place above T_g . If left long enough, the reptation of the mobilized chains will disentangle them from the crosslinks and lead to complete relaxation. However in the first instance, just above the T_g , it would be expected that this process would be relatively slow and that the stretched network would be retained. The linear length of the chains between crosslinks (i.e. the entanglement molecular weight in an amorphous linear polymer) is much longer than the distance between crosslinks in the undeformed solid. Hence for a modest λ of 2, the distribution of segment directions in the relaxed chain configuration will be only slightly perturbed from that in the original undeformed sample. The observed near uniform diffraction halo (e.g. frame 54 in Figure 1) is quite consistent with this scenario. Thus the relaxation in orientation monitored by diffraction can be understood in terms of a change from a distribution of pseudo-affinely oriented segments to a configuration of segments associated with an effective rubber network.

Although the diffraction observations are in good qualitative agreement with the two deformation schemes, it is of interest to explore how well the deformations agree quantitatively on the basis of the approximation that the azimuthal extension of the equatorial arcs in patterns like those in frames 39 and 49 in Figure 1 is directly linked with the segment orientation. Figure 8 shows the predictions from the two models for the segment distributions after a λ of 2, using a value of $n=10$ in the Roe and Krigbaum¹⁷ relationship. This is typical of that deduced for poly(ethylene terephthalate) (PET); we are not aware of any literature values for PEEK.

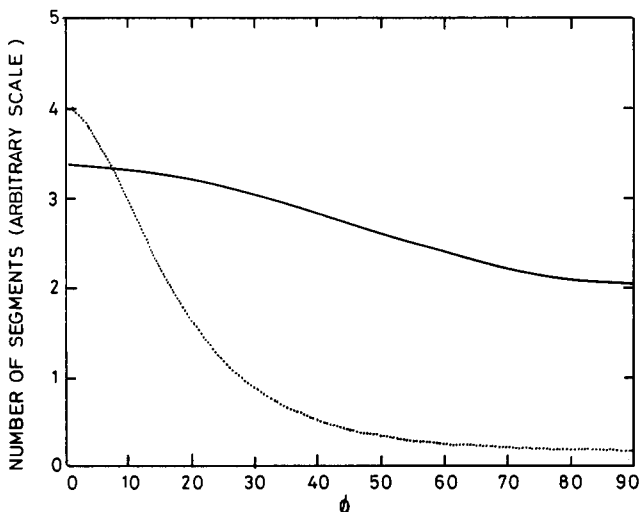


Figure 8 Predicted orientation distribution of chain segments for draw ratio 2 and 10 links per chain for a pseudo-affine deformation (.....) and a rubber network (—) ($\phi=0^\circ$ corresponds to meridional and 90° to equatorial)

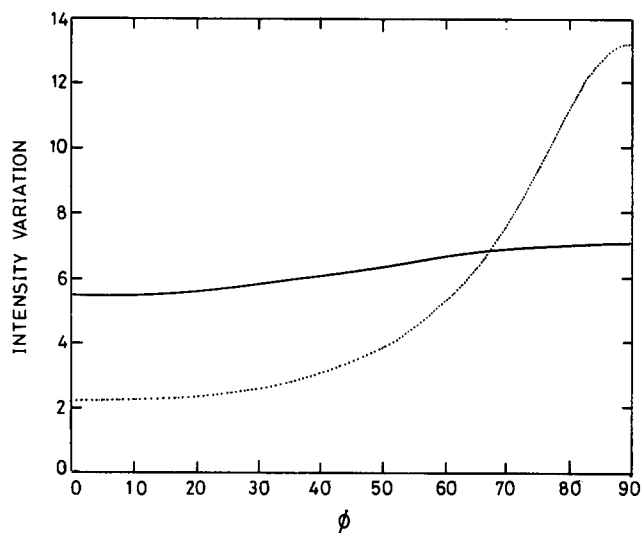


Figure 9 Predicted distribution of azimuthal scatter from segments for draw ratio 2 for a pseudo-affine deformation (.....) and a stretched rubber network (—) ($\phi=0^\circ$ corresponds to meridional and 90° to equatorial)

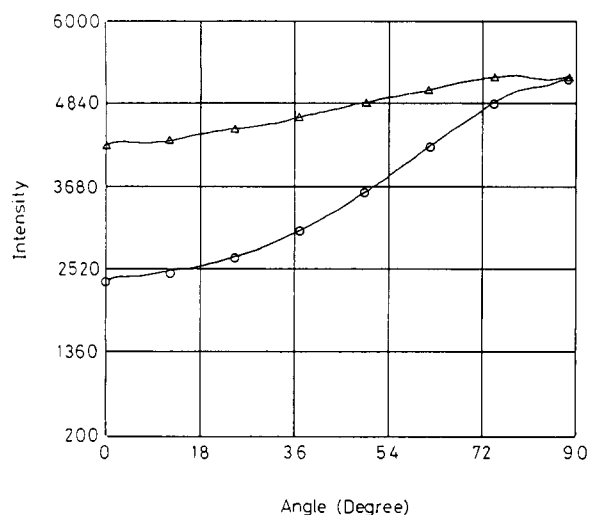


Figure 10 Experimental azimuthal scans for an interrupted experiment for frame 1 (O) recorded at 52°C and frame 50 (Δ) recorded at 153°C

These distributions have been transformed using the convolution procedure described by Mitchell and Windle⁹ to give the predicted diffraction profiles in Figure 9. Figure 10 shows experimental scans taken from frames 1 and 50 of the interrupted experiment summarized in Figures 3 and 4. The modulation in intensity between the 0° and 90° directions of the network model agrees well with the observed profile for frame 50. However, although there is a much enhanced intensity on the equator in frame 1, the modulation is a poor match for that predicted for the pseudo-affine model. This poor agreement does not invalidate the model but is an indication of the weakness of the approximation that the azimuthal extension of the arcs in such patterns directly maps out the segment orientation. The problem has been considered by Mitchell¹⁹.

The final stage to consider is the appearance of an oriented crystalline component when the temperature is raised further beyond T_g . The crucial point that needs to be explained is why the orientation of the crystals is so much higher than the orientation of the amorphous

segments from which they grew. Since this crystallization is occurring above the T_g where co-operative segment motions are able to take place, it follows that crystallization from an oriented melt state is being observed here. This situation has been extensively discussed in the literature²⁰. It has been established that a key mechanism for this process is row nucleation; this involves first the formation of a highly oriented fibrillar nucleus followed by the growth of lamellae on to the central fibril giving rise to so-called shish kebab structures²¹. In this way, the overall crystalline chain orientation is governed by the orientation of the original thread nuclei. Studies of this crystallization process have shown that the central fibril can itself consist of a periodic array of crystals along the fibril. The lateral development of the subsequent lamellae will depend on the concentration of the nuclei which will in turn depend on the drawing conditions. If the concentration is very high then lateral development of the lamellae will be restricted. In the limit it could become arguable whether significant lamellar growth occurs at all. The SAXS data are directly relevant to this issue.

The meridional diffraction peak at 140 Å which developed in the SAXS as the temperature was raised above T_g (e.g. frame 34 in *Figure 5*) is a consequence of the periodicity of the correlated sequence of crystallites along the fibrillar growths. However, in the early stages the diffraction is in the form of a monotonically reducing intensity. This effect has also been seen at the start of crystallization from an isotropic melt and is consistent with diffraction from isolated lamellae. It is only after infilling with further lamellae that a periodic correlation is established which gives rise to a diffraction maximum. The considerable broadening of these diffraction spots seen in the lateral scans of *Figure 7* indicates that the crystallites are very narrow in the direction perpendicular to the draw direction. It suggests that in the present case the lamellar overgrowth is very limited and the structures are essentially fibrillar in nature. Furthermore, the fact that the lateral spread is essentially constant from the very earliest detected diffraction indicates that lateral development of the initial isolated crystals is as small as 100 Å.

Of particular importance here is why the initial nuclei are so well oriented. These nuclei will be predominantly associated with chain lengths in the entangled network which are stretched out so that they incorporate significant straightened sequences in a crystallographic conformation. Since these straight chains will be predominantly aligned along the principal strain axis it follows that the direction of the subsequent crystal growth will also be along the strain axis. It is important to note that the stretched out chains will most likely belong to the high molecular weight fraction of the molecular weight distribution. These will be the ones that take the longest time to reptate and relax out of the entanglements and will therefore emerge as the more efficiently oriented. They will be effectively diluted by the lower molecular weight species which can disentangle more quickly. Thus the chains which can operate more efficiently as nucleating sites upon further heating would not be expected to dominate the otherwise near isotropic WAXS pattern coming from the majority of the chain segments.

The above observations could have important implications for the mechanism of stress crystallization during

cold drawing. When polymers such as PEEK and PET are drawn below their T_g , highly oriented crystals appear when λ exceeds ~ 2.5 . This crystallization would appear to be a continuous process and it is normally not possible to distinguish distinct stages in the process. In the present experiments the drawing was stopped at a λ of 2, i.e. at a ratio below which crystallization is detected. It is tempting to propose that the intermediate relaxed state observed in this experiment also represents an important intermediate stage in the general case of crystallization during cold drawing. Namely, that the crystallization does not occur directly as a result of the pseudo-affine cold drawing (e.g. by the deforming segments being aligned crystallographically) but does so only after segmental mobility has occurred to enable the crystallization to occur within a local rubber network. From this viewpoint the crystallization process during cold drawing can be seen to be in essence identical to crystallization from an oriented melt state. This mechanism is also more acceptable from the point of view of normal crystallization where high segmental mobility is seen as a key part of the organization of chains into crystallographic register. It is a particular aim of our ongoing experiments to explore this proposition by resolving the cold drawing process in real time.

Finally, an explanation is needed for the curious effect seen in both experiments where the overall intensity over all azimuthal angles for the disoriented state just above the T_g is higher than in the precursor oriented state. One possibility is that this is a consequence of the low aspect ratio of the cold drawn film, which due to sideways restraint of the clamps results in an orientation that does not have pure fibre symmetry about the draw direction. Such a lack of fibre symmetry has been seen in previous studies of crystallized oriented PEEK, where it was found that there was a preference for the {200} crystal planes of PEEK to align parallel to the plane of the film sample²². If a similar preferred orientation occurs in the cold drawn amorphous sample then when viewed with the X-ray beam perpendicular to the film plane there will be a diminished scattered intensity. When the disorientation occurs at the T_g , there would be a gain in observable scatter if the segments become more randomized relative to the film plane.

However, this explanation does not explain the subsequent fall in intensity in the experiments of the interrupted type (*Figure 4*) above the T_g but before the appearance of crystallinity. In this case there is no significant change in the azimuthal intensity profile, suggesting that the change in intensity level could be a genuine result of the change in the relative disposition of neighbouring segments during the reorientation process at T_g . This phenomenon also needs further investigation.

CONCLUSIONS

The high brilliance of the SERC Daresbury SRS has been used in time-resolved X-ray diffraction studies to reveal novel behaviour by the thermoplastic polymer, PEEK, in which molecular orientation present as a result of cold drawing is apparently lost and subsequently recovered during a heating programme. The observations made around the T_g are interpreted in terms of two models by Kuhn and Grun which are taken to describe, respectively, behaviour of a polymer below and above its glass transition. The specific result in which the diffuse, almost

isotropic WAXS halo transforms around the T_g into a highly oriented crystalline pattern is consistent with a row nucleation process. However, the degree of lateral spread in the SAXS pattern indicates that the lateral development of the crystals is very limited even for those crystals that start to grow from the earliest stages of crystallization.

ACKNOWLEDGEMENTS

We wish to thank Professor I. M. Ward for advice on orientation processes in amorphous polymers. This work was supported by SERC Grants GR/F49330 (to WF, AM, RJO and DJB) and GR/H67966 (to WF, AM, RJO and DJB) and allocation of beam time on the SERC Daresbury Synchrotron Radiation Source.

REFERENCES

- 1 Zachmann, H. G. and Schmidt, G. F. *Makromol. Chem.* 1962, **52**, 23
- 2 Spruiell, J. E., McCord, D. E. and Beuerlein, R. A. *Trans. Soc. Rheol.* 1972, **16**, 535
- 3 Cakmak, M., Spruiell, J. E., White, J. L. and Lin, J. S. *Polym. Eng. Sci.* 1987, **27**, 893
- 4 Siesler, H. W. *Appl. Spectrosc.* 1985, **39**, 761
- 5 Elsner, G., Zachmann, H. G. and Milch, J. R. *Makromol. Chem., Rapid Commun.* 1981, **182**, 657
- 6 Gehrke, R., Riekel, C. and Zachmann, H. G. *Polymer* 1989, **30**, 1582
- 7 Mahendrasingam, A., Forsyth, V. T., Hussain, R., Greenall, R. J., Pigram, W. J. and Fuller, W. *Science* 1986, **223**, 195
- 8 Mahendrasingam, A., Fuller, W., Forsyth, V. T., Oldman, R. J., MacKerron, D. and Blundell, D. J. *Rev. Sci. Instrum.* 1992, **63**, 1087
- 9 Mitchell, G. R. and Windle, A. H. in 'Developments in Crystalline Polymers' (Ed. D. C. Bassett), 2nd Edn, Elsevier, London, 1988
- 10 Windle, A. H. in 'Developments in Oriented Polymers' (Ed. I. M. Ward), Vol. 1, Applied Science, London, 1982
- 11 Alexander, L. E. 'X-ray Diffraction Methods in Polymer Science', Wiley Interscience, New York, 1969
- 12 Biangardi, H. J. *J. Polym. Sci., Polym. Phys. Edn* 1980, **18**, 903
- 13 Von Falkai, B., Spilgies, G. and Biangardi, H. J. *Angew. Makromol. Chem.* 1982, **41**, 108
- 14 Blundell, D. J., Chivers, R. A., Curson, A. D., Love, J. C. and MacDonald, W. A. *Polymer* 1988, **29**, 1459
- 15 Doi, M. and Edwards, S. F. 'Theory of Polymer Dynamics', Clarendon Press, Oxford, 1986
- 16 Kuhn, W. and Grun, F. *Kolloid Z.* 1942, **101**, 248
- 17 Roe, R. J. and Krigbaum, W. R. *J. Appl. Phys.* 1964, **35**, 2215
- 18 Ward, I. M. *Br. J. Appl. Phys.* 1967, **18**, 1165
- 19 Mitchell, G. R. IUPAC Symposium on Non-crystalline Order in Polymers, Naples, 1985, p. 73
- 20 Keller, A. and Machin, M. J. *J. Macromol. Sci. (Phys.)* 1967, **B1**, 41
- 21 Barham, P. and Keller, A. *J. Mater. Sci.* 1985, **20**, 2281
- 22 Fuller, W., Oates, C. R., Mahendrasingam, A., Forsyth, V. T., Pigram, W. J., Greenall, R. J., Oldman, R. J., Barry, M. J. and Blundell, D. J. *Inst. Phys. Conf. Ser.* 1989, No. 101, p. 213